Journal of Materials Chemistry C

PAPER

View Article Online
View Journal | View Issue



Cite this: J. Mater. Chem. C, 2014, 2, 3936

# Fluorescent aggregates of hetero-oligophenylene derivative as "no quenching" probe for detection of picric acid at femtogram level†

Sharanjeet Kaur, Vandana Bhalla,* Varun Vij and Manoj Kumar*

Received 19th December 2013
Accepted 19th March 2014

DOI: 10.1039/c3tc32516d

www.rsc.org/MaterialsC

Fluorescent aggregates of hetero-oligophenylene derivative **3** serve as a "no quenching" probe for the detection of picric acid (PA) in aqueous media. Photo-induced intermolecular excited-state proton transfer from PA to pyridyl nitrogen results in the formation of protonated species, which exhibit emission at a different wavelength; hence, there is "no quenching" detection of PA in aqueous media.

## Introduction

Among various nitroaromatics, picric acid (PA) is a health hazard as it can cause skin/eye irritation and can affect the organs involved in the respiratory system.[1,2] PA is a strong organic acid,[3] and its vapors are hazardous and cause headache, weakness, anemia and liver injury.[4] Furthermore, with the its electron-deficient character, the degradation of PA is more difficult in the biosystem, which is probably responsible for many chronic diseases such as sycosis and cancer.[5] PA is also used in dye manufactures, pharmaceuticals, and chemical laboratories.[6,7] Like many polynitrated aromatic compounds, it is a powerful explosive and its explosive nature is equivalent to 105% of trinitrotoluene (TNT).[8,9] Further, because of its high solubility in water, it can easily contaminate soil and groundwater when exposed. As a result, there have been considerable efforts for development of cost-efficient, selective,[10,11] sensitive, fast and portable detection methods for PA in aqueous media.[12–15] Thus, various fluorescent materials have been developed that serve as turn-off sensors for PA.[16–22] However, fluorescent sensors showing no quenching response are attractive due to less interference from fluctuation of background fluorescence,[23] but fluorescent materials showing no quenching response towards nitroaromatics are still in their infancy.[24,25] Motivated by better sensitivity and reliability of "no quenching" sensors, we were interested in the development of fluorescent assemblies showing a "no quenching" response towards PA.

Recently, stimuli-responsive smart materials with tunable photophysical properties have attracted considerable research interest.[26] Keeping this in view, we designed and synthesized hetero-oligophenylene derivative **3** having pyridine groups for the sensitive detection of PA. Pyridine exhibits Lewis basicity and is a good proton acceptor. On the other hand, electron-deficient PA has an acidic character. We envisaged that formation of protonated species due to intermolecular transfer of protons from PA to the pyridine group of derivative **3** could influence the photophysical properties of the system. Interestingly, derivative **3** forms fluorescent aggregates in aqueous media and exhibits reversible photo-induced intermolecular excited-state proton transfer from PA to pyridine nitrogen of aggregates of derivative **3** and subsequent formation of protonated species exhibited emission at different wavelengths; hence, a "no quenching" response towards PA was observed in aqueous media. The fluorescent aggregates of derivative **3** serve as a better probe for detection of PA in comparison with the previously reported chemosensors for PA.[27] To the best of our knowledge, this is the first report where fluorescent aggregates of hetero-oligophenylene derivative **3** serve as "no quenching" chemosensors for PA based on a photo-induced, intermolecular excited-state proton transfer mechanism with a detection limit at the femtogram level.

## Results and discussion

The target compound **3** was synthesized *via* Diels–Alder reaction of 3-(2-(pyridine-3-yl)ethynyl)pyridine **1a** (ref. 28) with 2,5-diphenyl-3,4-di(pyridin-2-yl)cyclopenta-2,4-dienone **2a** (ref. 29) in diphenylether at 240 °C in 70% yield (Scheme 1). The $^1$H NMR spectrum of compound **3** showed five doublets at 8.16, 8.12, 7.24, 7.17 and 7.02 ppm, one singlet at 8.08 ppm, one multiplet at 6.83–6.91 ppm and one triplet at 6.8 ppm corresponding to aromatic protons. A parent ion peak for $(M + H^+)$ was observed at $m/z$ 539.2302 in ESI mass spectrum (pS15 to S17 in ESI†). These spectroscopic data corroborate the structure **3** for this compound. To get insight into the role played by 3-pyridyl/2-pyridyl groups in the "no quenching" response, we also

*Department of Chemistry, UGC-Centre for Advanced Studies-1, Guru Nanak Dev University, Amritsar, Punjab, India. E-mail: vanmanan@yahoo.co.in; mksharmaa@yahoo.co.in*

† Electronic supplementary information (ESI) available: Synthesis of compound **3** and **5**, characterization data, UV-vis and fluorescence studies. See DOI: 10.1039/c3tc32516d

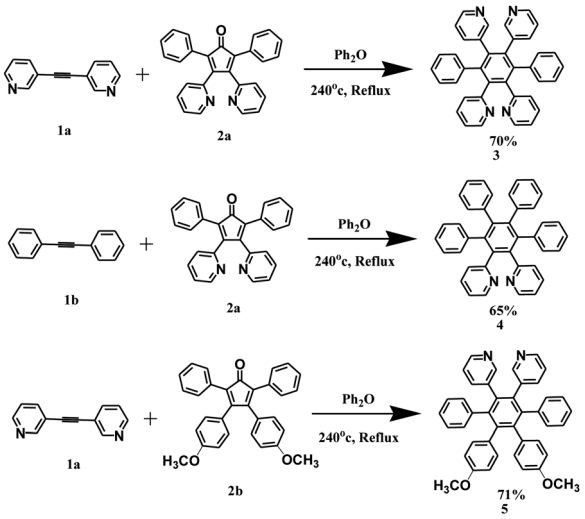


Scheme 1 Synthesis of compounds **3–5**.

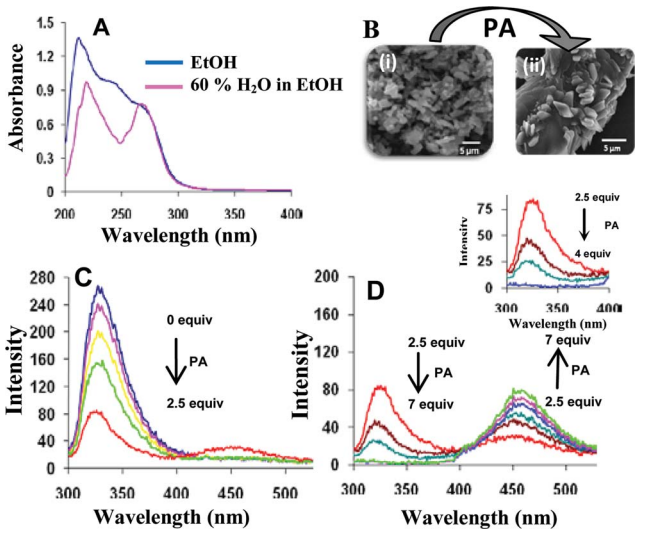


Fig. 1 (A) UV-vis absorption spectra of **3** (50 μM) in EtOH and $H_2O$–EtOH (6 : 4) buffered with HEPES, pH = 7.0. (B) (i) Scanning electron microscopy (SEM) image of aggregates of compound **3** ($10^{-4}$ M) in $H_2O$–EtOH (6 : 4) buffered with HEPES, pH = 7.0. (ii) SEM image of derivative **3** ($10^{-4}$ M) in presence of 7 equiv. of PA in $H_2O$–EtOH (6 : 4) buffered with HEPES pH = 7. (C) Fluorescence emission spectra of **3** (50 μM) with the addition of picric acid (125 μM) in $H_2O$–EtOH (6 : 4) buffered with HEPES, pH = 7.0; $\lambda_{ex}$ = 273 nm. (D) Fluorescence emission spectra of derivative **3** (50 μM) up to the addition of 350 μM of PA in $H_2O$–EtOH (6 : 4) buffered with HEPES pH = 7; $\lambda_{ex}$ = 273 nm. Inset shows the emission band at 339 nm completely quenched with the addition of 200 μM of PA.

synthesized hetero-oligophenylene derivatives **4** and **5** (ref. 28) as model compounds incorporating 2-pyridyl and 3-pyridyl groups, respectively. The derivative **4** was synthesized by Diels–Alder reaction of 1,2-diphenylethyne **1b** (ref. 30) with 2,5-diphenyl-3,4-di(pyridin-2-yl)cyclopenta-2,4-dienone **2a** (ref. 29) in diphenylether at 240 °C in 65% yield (Scheme 1). The $^1$H NMR spectrum of compound **4** showed two doublets at 8.13 and 6.98 ppm, one triplet at 7.19 ppm and one multiplet at 6.73–6.86 ppm corresponding to aromatic protons. A parent ion peak for ($M + H^+$) was observed at *m*/*z* 537.2332 in ESI mass spectrum (pS18 to S20 in ESI†). The derivative **5** was prepared by the reported method.[28]

The UV-vis spectrum of compound **3** in EtOH exhibits an absorption band at 213 nm with two shoulders at 245 nm and 271 nm (Fig. 1A). On addition of water (60% volume fractions) to the EtOH solution of derivative **3**, the absorption band at 213 nm is slightly red shifted to 220 nm and a well-defined absorption band appeared at 271 nm. The red shifting of the absorption band indicates aggregation of derivative **3** to produce J-type assemblies.[31,32] Since it is known that deaggregation takes place on increasing the temperature,[33] we carried out temperature-dependent UV-vis studies of derivative **3** in $H_2O$–EtOH (6 : 4). It was observed that, with an increase in temperature up to 70 °C, the absorption band at 220 nm blue shifted to 213 nm (Fig. S1 in ESI†). This revival of an absorption band at 213 nm clearly indicates the deaggregation of J-type assemblies. To further prove the formation of J-assemblies, we carried out concentration-dependent $^1$H NMR studies of derivative **3** in $CDCl_3$ (Fig. S2 in ESI†). These studies show the upfield shifting of signals corresponding to aromatic protons. Such an upfield shift is attributed to the intermolecular shielding from the neighboring aromatic molecules, suggesting their tendency to undergo self-association to form aggregates.[34] The scanning electron microscopy (SEM) image of compound **3** in the solvent mixture of $H_2O$–EtOH (6 : 4) shows the presence of aggregates [Fig. 1B(i)]. The solution of aggregates is visibly transparent and stable at room temperature for several weeks.

Derivative **3** in $H_2O$–EtOH (6 : 4) exhibits fluorescence emission at 339 nm ($\Phi_F$ = 0.35)[35] when excited at 273 nm (Fig. 1C). The strong emission of aggregates of derivative **3** prompted us to explore their potential application as chemosensor for the detection of nitro derivatives such as trinitrotoluene (TNT), trinitrobenzene (TNB), picric acid (PA), *etc.* Thus, we carried out the fluorescence titrations of aggregates of compound **3** in $H_2O$–EtOH (6 : 4) toward various nitro derivatives such as picric acid (PA), 2,4,6-trinitrololuene (TNT), 2,4-dinitrotoluene (DNT), 1,4-dinitrobenzene (DNB), 1,4-benzoquinone (BQ), nitromethane (NM), and 2-nitrotoluene (NT). Upon addition of PA up to 2.5 eq. to the solution of derivative **3** in the $H_2O$–EtOH (6 : 4) mixture, the intensity of emission band at 339 nm decreased gradually and a new band appeared at 446 nm (Fig. 1C). On addition of PA up to 4 eq., the intensity of emission band at 339 nm quenched completely (inset, Fig. 1D) and the intensity of emission band at 446 nm increased (Fig. 1D). On further addition of PA up to 7 eq., the intensity of emission band at 446 nm increased along with a red shift of 14 nm to give final emission at 460 nm (Fig. 1D). The formation of a new band at 460 nm suggests the formation of protonated species due to excited-state intermolecular proton transfer from PA to pyridyl nitrogen. The factor responsible for this transfer is the matching of the acidity of the phenolic group of PA with the basicity of the pyridine group in the excited state.

On the other hand the absorption studies of derivative **3** aggregates in the presence of PA do not suggest formation of protonated species in the ground state (Fig. S3 in ESI†). The

absorption studies of derivative **3** aggregates in the presence of 7 eq. of PA show the appearance of a band at 356 nm corresponding to PA (Fig. S4 in ESI†) and an increase in absorption intensity of the band at 218 nm, whereas slight change in the intensity of absorption band at 273 nm is observed (Fig. S3 in ESI†). However, the fluorescence spectrum of the same solution shows the formation of a new band at 460 nm (Fig. S5 in ESI†). Thus, the absorption studies rule out the charge transfer interactions between aggregates of derivative **3** and PA in the ground state. On the basis of fluorescence studies of aggregates of **3** in the presence of PA, we propose that the sensing mechanism involves two steps (Fig. 2). In the first step, interaction between the aggregates of **3** and PA takes place, which is responsible for quenching of the emission band at 339 nm (Fig. 1C and inset Fig. 1D). In the next step, we believe that upon light absorption, the basicity of pyridyl nitrogen is enhanced,[36] which facilitates proton transfer from PA to pyridyl nitrogen in the excited state. This excited-state intermolecular proton transfer from PA to pyridine groups leads to the formation of protonated species, which is responsible for appearance of the new band at 460 nm (Fig. 1D). Further, we determined the p$K_a$ of picric acid in $H_2O$–EtOH (6 : 4) solution buffered with HEPES at pH = 7 using the UV-vis spectroscopic method,[37,38] and it comes out to be 6.45 (Fig. S6 and PS6 in ESI†). This result shows that the presence of a significant portion of picric acid in its conjugate acid form supports the proposed mechanism. To further support our theory of the mechanism, we carried out absorption and emission studies of derivative **3** in acetonitrile with PA (the p$K_a$ of PA in acetonitrile is 11),[39] and similar absorption and emission results were obtained that suggest the formation of protonated species due to excited-state intermolecular proton transfer from PA to pyridyl nitrogen (Fig. S8 in ESI†). Further, we recorded the $^1$H NMR spectrum of derivative **3** in a solvent mixture of $D_2O$–$CD_3OD$ (6 : 4) in the presence of PA, which shows an average downfield shift of 0.05 ppm in signals corresponding to aromatic protons (Fig. S9 in ESI†). This very low downfield shift in the signal corresponding to aromatic protons indicates the very little charge transfer interaction between derivative **3** and PA. However, the considerable spectral overlap between the emission spectrum of aggregates of derivative **3** and the absorption spectrum of PA indicates the possibility of energy transfer between aggregates and molecules of PA (Fig. S10 in ESI†). Thus the quenching of the emission band at 339 nm is due to energy transfer and very little charge transfer interaction between aggregates of derivative **3** and PA. To confirm the excited-state intermolecular proton transfer, we carried out fluorescence studies of aggregates of derivative **3** with trifluoroacetic acid (TFA), which is strong non-aromatic acid, under the same set of conditions as was used for PA. The emission spectra show the appearance of an emission band at 439 nm upon addition of 1.5 μL of TFA ($10^{-1}$ M), which confirms the protonation of pyridyl nitrogen of derivative **3** aggregates in the excited state (Fig. S11 in ESI†). Interestingly, no significant quenching of the emission band at 339 nm was observed. Thus the nature of interaction between aggregates of derivative **3** and PA is considerably different from that for other acidic molecules. Furthermore, the emission signal corresponding to protonated species is more red shifted in the presence of PA ($\Delta\lambda = 121$ nm) (Fig. 1C) as compared with that in the presence of TFA ($\Delta\lambda = 100$ nm) (Fig. S11 in ESI†). We believe that in comparison with electron-deficient and acidic PA, TFA has only an acidic character, and thus a different sensing response is observed. We recorded the absorption spectra of aggregates of derivative **3** in $H_2O$–EtOH (6 : 4) in the presence of TFA (Fig. S12 in ESI†). No new band corresponding to the protonated species was observed, which also confirms that protonation of aggregates is an excited-state phenomenon (Fig. S12 in ESI†). Further, we also carried out fluorescence titration of derivative **3** after protecting the hydroxyl group of PA with the methoxy group (Fig. S13 in ESI†) and, interestingly, no new band appeared. However, there is only quenching of the emission band at 339 nm. These studies clearly indicate that the formation of an emission band at 460 nm is due to excited-state intermolecular proton transfer from PA to pyridyl nitrogen. To confirm that the protonation of aggregates of derivative **3** is not a ground-state phenomenon, we studied the effect of triethylamine on emission spectra of aggregates of derivative **3** in the presence of PA. The addition of 8 equiv. of triethylamine ($10^{-2}$ M) results in gradual weakening of the band at 460 nm; however, the emission band at 339 nm was not revived (Fig. S14 in ESI†). In contrast, no significant change was observed in the absorption spectra of aggregates of derivative **3** in the presence of PA with the addition of triethylamine (Fig. S15 in ESI†). These results further confirm that the protonation of aggregates of derivative **3** is an excited-state phenomenon and the protonated species cannot be observed in the ground state. Further the SEM

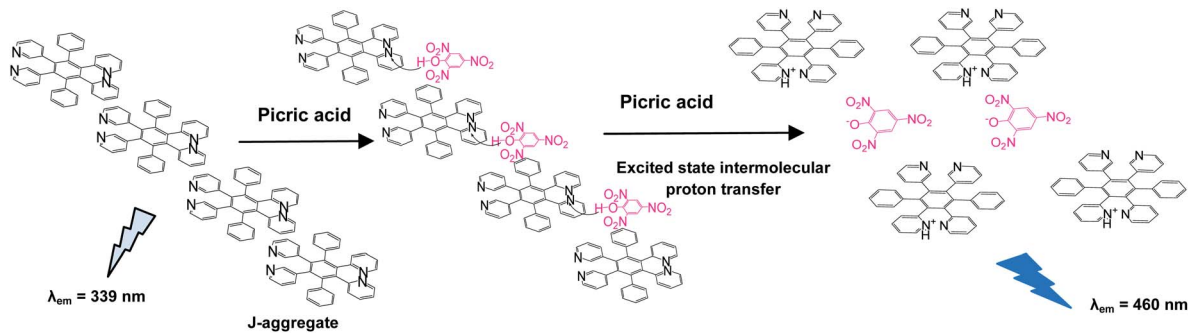


Fig. 2 Mechanism of the recognition behavior of aggregates of **3** towards picric acid in $H_2O$–EtOH (6 : 4).

 

image of derivative **3** in $H_2O$–EtOH (6 : 4) in the presence of 7 equiv. of PA shows layered flakes, thus indicating modulation of a self-assembled structure of derivative **3** on addition of PA [Fig. 1B(ii)].

Under the same set of conditions as was used for the detection of PA, we also carried out fluorescence studies of aggregates of derivative **3** in presence of NT (40 equiv.), DNT (62 equiv.), TNT (65 equiv.), BQ (120 equiv.) and NM (135 equiv.), DNB (82 equiv.), but no new band corresponding to the protonated species was observed (Fig. S16 in ESI†). Further, we also carried out fluorescence studies of aggregates of derivative **3** with phenolic derivatives (catechol, Br-phenol, I-phenol, 2,4-dinitrophenol (DN), 4-nitrophenol (NP) and phenol) but no new band appeared at 460 nm upon titrations with phenolic derivatives; however, emission bands at 302 and 325 nm are the characteristic emission bands of phenol and catechol itself (Fig. S17 in ESI†). Thus, derivative **3** is selective towards PA and the "no quenching" response is observed only where PA exists among the various nitro and phenol derivatives tested (Fig. S18 in ESI†). The fluorescence lifetime studies of derivative **3** aggregates monitored at 339 nm show shorter decay time (0.606 ns); however, at 460 nm in the presence of PA (6 equiv.), a long-lived component (0.840 ns) is observed (Fig. S19 in ESI†). This result suggests the formation of a new fluorescent species due to interaction between derivative **3** and PA. The detection limit in this case was found to be 26 nM (Fig. S20 in ESI†). We also carried out pH studies and found that emission spectra of a derivative **3** solution in buffer–EtOH (6 : 4) mixture using a universal buffer is independent of pH in the range of 6 to 14 (Fig. 3A). Further, the effect of PA on derivative **3** at different pH values was also studied. At pH = 2 (acidic), the fluorescence spectra initially shows the emission band at 439 nm, and with the addition of 16 equiv. (0.8 mM) PA, the emission band at 439 nm shifted to a longer wavelength and finally reached emission at 460 nm, which corresponds to the protonated species (Fig. 3B). However, at pH = 12 (basic), the effect of PA on derivative **3** is same as that at neutral pH = 7. At acidic pH = 2, more PA equiv. are required for protonation because of already-protonated pyridyl groups, which slows down the transfer of protons from PA to pyridyl nitrogen (Fig. S21 in ESI†).

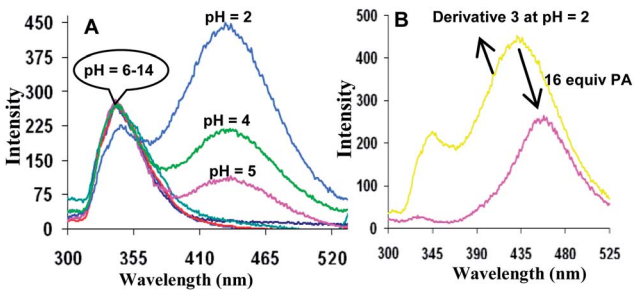


Fig. 3 (A) Fluorescence emission spectra of derivative **3** (50 μM) at different pH in universal buffer–EtOH (6 : 4); $\lambda_{ex}$ = 273 nm. (B) Fluorescence emission spectra of derivative **3** (50 μM) at pH = 2 with the addition of 16 equiv. (0.8 mM) of PA in $H_2O$–EtOH (6 : 4); $\lambda_{exc}$ = 273 nm.

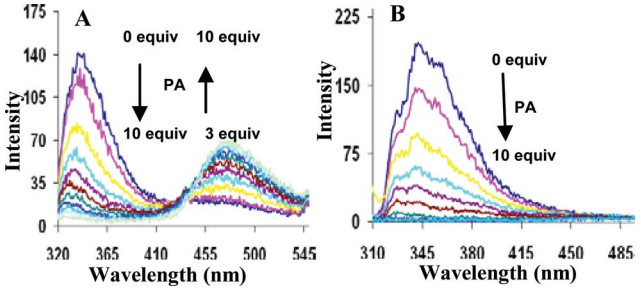


Fig. 4 (A) Fluorescence emission spectra of derivative **4** (50 μM) with the addition of picric acid (500 μM) in $H_2O$–EtOH (3 : 7) buffered with HEPES pH = 7; $\lambda_{exc}$ = 273 nm. (B) Fluorescence emission spectra of derivative **5** (5 μM) with the addition of picric acid in $H_2O$–EtOH (6 : 4) buffered with HEPES pH = 7; $\lambda_{exc}$ = 290 nm.

To study the role of 3-pyridyl/2-pyridyl groups in a "no quenching" response, we recorded the fluorescence spectra of derivatives **4** and **5** in the presence of PA. Both derivatives have rotors and form aggregates in aqueous media. Interestingly, a solution of derivative **4** having 2-pyridyl groups in $H_2O$–EtOH (3 : 7) mixture exhibits a "no quenching" response towards PA (Fig. 4A), whereas under the same set of conditions derivative **5** having 3-pyridyl groups exhibits quenching of emission in the presence of PA (Fig. 4B). No new band was observed in the case of derivative **5** having 3-pyridyl groups with the addition of PA, which suggests that the site of protonation is only in the 2-pyridyl groups. We also carried out fluorescence studies of derivative **5** in the presence of TFA; however, no significant change in the emission spectra was observed (Fig. S22 in ESI†). The SEM image of derivative **5** shows the presence of spherical aggregates (Fig. S23 in ESI†). It is expected that 3-pyridyl nitrogens will be present at the periphery and may be hydrogen bonded to the solvent molecules. We believe that the 3-pyridyl group has relatively weaker basicity that is not enough to enable the excited-state proton transfer. These results suggest the importance of 2-pyridyl groups for "no quenching" detection of PA in aqueous media.

Further, PA can contaminate the human body, clothing and other materials in the surroundings during the manufacture of rocket fuel and fireworks. Detection of these traces is a major concern in the field of analytical and forensic sciences. In this context, we prepared TLC strips by dip-coating a solution of aggregates of **3** onto TLC strips, followed by drying them in a vacuum in order to check for residual contamination in contact mode. We prepared several samples of solution-coated TLC strips and studied the response of their fluorescence towards picric acid in contact mode and solution phase. PA crystals were placed over coated TLC strips for 5 s to test the contact mode response of derivative **3** nanoflakes towards PA. Upon illumination with a UV lamp, blue spots were observed in the contact area [Fig. 5(i)(a) and (b)]. We also checked the effect of various concentrations of PA, DNT and TNT solutions on the fluorescent TLC strips by applying small spots of different concentrations of analytes to the TLC strips [Fig. 5(ii)(a)–(f)]. The minimum amount of PA detectable by the naked eye was as low as 10 μL of $1 \times 10^{-12}$ M solution, thereby registering a detection

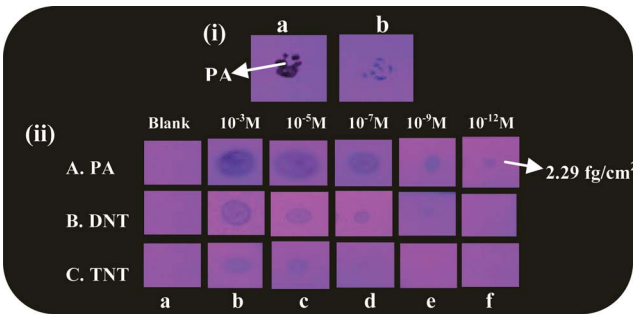


Fig. 5 Photographs of derivative-**3**-coated TLC strips under different experimental conditions. (i) (a) PA crystals on top of derivative-**3**-coated TLC strips; (b) removal of PA crystal after 5 s. (ii) Photographs of fluorescence quenching of derivative-**3**-coated TLC strips by PA, DNT and TNT in contact mode (10 μL of analyte with a contact area of 0.05 $cm^2$) when viewed under 365 nm UV illumination.

limit at the 2.29 femtogram level, whereas these TLC strips were not found to be sensitive towards DNT and TNT [Fig. 5(ii)(a)–(f)]. However, no visible quenching was observed by applying blank solvent (ethanol) on fluorescent paper strips [Fig. 5(ii)(a)].

## Conclusion

We designed and synthesized hetero-oligophenylene derivative **3**, which forms fluorescent aggregates in aqueous media; and these aggregates work as an efficient and selective "no quenching" fluorescent sensor for the detection of picric acid in solution and solid state. In addition, we prepared fluorescent TLC strips carrying derivative **3** aggregates that can detect the PA up to femtogram level.

## General experimental methods

All the fluorescence spectra were recorded on SHIMADZU 5301 PC spectrofluorometer. UV spectra were recorded on Shimadzu UV-2450PC spectrophotometer with a quartz cuvette (path length: 1 cm). The cell holder was thermostated at 25 °C. Elemental analysis was done using a Flash EA 1112 CHNS/O analyzer of Thermo Electron Corporation. $^1$H and $^{13}$C NMR spectra were recorded on a JEOL-FT NMR-AL 300 MHz spectrophotometer and Bruker (Avance II) FT-NMR 400 MHz spectrophotometer using $CDCl_3$ and DMSO-$d^6$ as solvent and tetramethylsilane ($Si(CH_3)_4$) for internal standards. Data are reported as follows: chemical shifts in parts per million ($\delta$), multiplicity (s = singlet, br = broad signal, d = doublet, m = multiplet), coupling constants (Hz), integration, and interpretation. All spectrophotometric titration curves were fitted with SPECFIT 32 software. All spectral characterizations were carried out in HPLC-grade solvents at 20 °C within a 10 mm quartz cell.

### Fluorescence quantum yield

9,10-Diphenylanthracene ($\phi_f = 0.95$) in ethanol has been used as standard in the measurement of fluorescence quantum yield by using eqn (1), in which $\phi_{fs}$ is the radiative quantum yield of the sample; $\phi_{fr}$ is the radiative quantum yield of the reference; As and Ar are the absorbance of the sample and the reference, respectively; $D_s$ and $D_r$ are the areas of emission for the sample and reference; $L_s$ and $L_r$ are the lengths of the absorption cells; and $N_s$ and $N_r$ are the refractive indices of the sample and reference solutions (pure solvents were assumed).

$$\phi_{fs} = \phi_{fr} \times \frac{1 - 10^{-ArLr}}{1 - 10^{-AsLs}} \times \frac{N_s^2}{N_r^2} \times \frac{D_s}{D_r} \quad (1)$$

### Experimental details of finding the detection limit

To determine the detection limit, fluorescence titration of compound **3** with picric acid was carried out by adding aliquots of a picric acid solution of micromolar concentration and plotting the fluorescence intensity as a function of picric acid. From this graph, the concentration at which there was a sharp change in the fluorescence intensity multiplied by the concentration of receptor gave the detection limit.

### Preparation of TLC strips

TLC strips (5 cm × 2 cm) were prepared by coating with derivative **3** ($50 \times 10^{-6}$ M), followed by removal of solvent in a vacuum at room temperature. The ensemble-coated filter papers were then cut into 8 pieces (1 cm × 1 cm) to get the test strips and used for the detection of explosives.

### Contact mode visual detection of PA

Aqueous samples were prepared by dissolving PA in EtOH. The explosive solutions were spotted onto the TLC strips at the desired concentration using a micropipette. A solvent blank was spotted near the spot of each explosive. In order to ensure consistent analysis, all depositions were prepared from a 10 μL volume, thereby producing a spot ~0.5 cm in diameter. After solvent evaporation, the filter paper was illuminated with 365 nm UV light. The blue-coloured spots (under UV light) were identified by an independent observer, and each set of experiments was repeated three times for consistency. The detection limits were calculated from the lowest concentration of the explosive that enabled an independent observer to detect the quenching visually.

## Experimental details

The compounds **1a**,[28] **2a**,[29] **1b**,[30] and **5** (ref. 28) were synthesized according to literature procedure.

### Synthesis of compound 3

A solution of 3-(2-(pyridin-3-yl)ethynyl)pyridine **1a** (ref. 28) (1.4 mmol) and 2,5-diphenyl-3,4-di(pyridin-2-yl) cyclopenta-2,4-dienone **2a** (ref. 29) (1.4 mmol) in diphenyl oxide (2 mL) was refluxed under an atmosphere of nitrogen. After 18 h, the reaction mixture was cooled to room temperature followed by the slow addition of hexane (5 mL) to the reaction mixture. The hexane was decanted off and the rest of the crude product was purified by column chromatography using $CHCl_3$–hexane (8 : 2) as eluent to give a beige solid (70%); $^1$H NMR (400 MHz, $CDCl_3$): $\delta$ = 8.16 [d, $J$ = 4 Hz, 2H, ArH], 8.12 [d, $J$ = 4 Hz, 2H, ArH], 8.08

 

[s, 2H, ArH], 7.24 [d, $J = 4$ Hz, 2H, ArH], 7.17 [d, $J = 4$ Hz, 2H, ArH], 7.02 [d, $J = 4$ Hz, 2H, ArH], 8.08 [s, 2H, ArH], 6.83–6.91 [m, 10H, ArH], 6.8 [t, $J = 4$ Hz, 2H, ArH]; $^{13}$C NMR (100 MHz, $CDCl_3$): 158.25, 151.55, 151.27, 147.88, 146.98, 140.87, 138.68, 138.31, 138.10, 137.79, 134.7, 130.86, 127.37, 127.04, 126.54, 126.19, 122.26, 120.66; ESI-MS: calculated: 538.2157; found: 539.2302 $(M + 1)^+$; elemental analysis: calcd for $C_{38}H_{26}N_4$: C 84.73; H 4.87; N 10.40; found: C 84.41%; H 4.72%, N 10.15%.

### Synthesis of compound 4

A solution of 1,2-diphenylethyne **1b** (ref. 30) (1.4 mmol) and 2,5-diphenyl-3,4-di(pyridin-2-yl) cyclopenta-2,4-dienone **2a** (ref. 29) (1.4 mmol) in diphenyl oxide (2 mL) was refluxed under an atmosphere of nitrogen. After 18 h, the reaction mixture was cooled to room temperature followed by the slow addition of hexane (5 mL) to the reaction mixture. The hexane was decanted off and the rest of the crude product was purified by column chromatography using $CHCl_3$–hexane (8 : 2) as eluent to give a beige solid (65%); $^1$H NMR (400 MHz, $CDCl_3$): $\delta = 8.13$ [d, $J = 4$ Hz, 2H, ArH], 7.19 [t, $J = 4$ Hz, 2H, ArH], 6.98 [d, $J = 4$ Hz, 2H, ArH], 6.73–6.86 [m, 22H, ArH]; $^{13}$C NMR (100 MHz, $CDCl_3$): 120.29, 125.37, 125.49, 126.63, 126.71, 131.14, 131.27, 134.44, 139.71, 140.12, 141.21, 147.66; ESI-MS: calculated: 536.2252; found: 537.2332 $(M + 1)^+$; elemental analysis: calcd for $C_{40}H_{28}N_2$: C 89.52; H 5.26; N 5.22; found: C 89.31%; H 5.01%, N 5.11%.

## Acknowledgements

We are thankful to DST (ref. no. SR/S1/OC-63/2010 and SR/S1/OC-69/2012) and CSIR (ref. no. 02(0083)/12/EMR-II) for financial support. SK is thankful to the "UGC-BSR" Scheme for providing a fellowship.

## Notes and references

1 Safety Data Sheet for Picric Acid, Resource of UK National Institute of Health.
2 P. C. Ashbrook and T. A. Houts, *ACS Division of Chemical Health and Safety*, 2003, **10**, 27.
3 G. V. Perez and A. L. Perez, *J. Chem. Educ.*, 2000, **77**, 910.
4 R. L. Woodfin, *Trace Chemical Sensing of Explosives*, John Wiley & Sons Inc., 2007.
5 J. Shen, J. Zhang, Y. Zuo, L. Wang, X. Sun, J. Li, W. Han and R. He, *J. Hazard. Mater.*, 2009, **163**, 1199.
6 D. T. Meredith and C. O. Lee, *J. Am. Pharm. Assoc.*, 1939, **28**, 369.
7 E. H. Volwiler, *Ind. Eng. Chem.*, 1926, **18**, 1336.
8 J. Akhavan, *Chemistry of Explosives*, Royal Society of Chemistry, 2nd edn, 2004.
9 P. Cooper, *Explosive Engineering*, Wiley-VCH, 1996, p. 33.
10 X. Yang, C. J. Niu, G. L. Shen and R. Q. Yu, *Analyst*, 2001, **126**, 349.
11 C. Jian and W. J. Seit, *Anal. Chim. Acta*, 1990, **237**, 265.
12 S. J. Toal and W. J. Trogler, *J. Mater. Chem.*, 2006, **16**, 2871.
13 D. Li, J. Liu, R. T. K. Kwok, Z. Liang, B. Z. Tang and J. Yu, *Chem. Commun.*, 2012, **48**, 7167.
14 S. Shanmugaraju, H. Jadhav, Y. P. Patil and P. S. Mukherjee, *Inorg. Chem.*, 2012, **51**, 13072.
15 L. Ding, Y. Liu, Y. Cao, L. Wang, Y. Xin and Y. Fang, *J. Mater. Chem.*, 2012, **22**, 11574.
16 S. S. Nagarkar, B. Joarder, A. K. Chaudhari, S. Mukherjee and S. K. Ghosh, *Angew. Chem., Int. Ed.*, 2013, **52**, 2881.
17 J. D. Xiao, L. G. Qiu, F. Ke, Y. P. Yuan, G. S. Xu, Y. M. Wanga and X. Jiang, *J. Mater. Chem. A*, 2013, **1**, 8745.
18 S. Kumar, N. Venkatramaiah and S. Patil, *J. Phys. Chem. C*, 2013, **117**, 7236.
19 B. Roy, A. K. Bar, B. Gole and P. S. Mukherjee, *J. Org. Chem.*, 2013, **78**, 1306.
20 N. Venkatramaiah, S. Kumar and S. Patil, *Chem. Commun.*, 2012, **48**, 5007.
21 T. Liu, L. Ding, G. He, Y. Yang, W. Wang and Y. Fang, *ACS Appl. Mater. Interfaces*, 2011, **3**, 1245.
22 M. E. Germain and M. J. Knapp, *J. Am. Chem. Soc.*, 2008, **130**, 5422.
23 A. Barba-Bon, A. M. Costero, S. Gil, M. Parra, J. Soto, R. Martınez-Manez and F. Sancenon, *Chem. Commun.*, 2012, **48**, 3000.
24 Y. Xu, B. Li, W. Li, J. Zhao, S. Sun and Y. Pang, *Chem. Commun.*, 2013, **49**, 4764.
25 J. C. Sanchez and W. C. Trogler, *J. Mater. Chem.*, 2008, **18**, 3143.
26 M. Irie, T. Fukaminato, T. Sasaki, N. Tamai and T. Kawai, *Nature*, 2002, **420**, 759.
27 For comparison with reported PA sensors, see ESI,Table S1,† page S21.
28 V. Bhalla, V. Vij, A. Dhir and M. Kumar, *Chem.–Eur. J.*, 2012, **18**, 3765.
29 Z. Li, L. Zhang, L. Wang, Y. Guo, L. Cai, M. Yu and L. Wei, *Chem. Commun.*, 2011, **47**, 5798.
30 M. J. Mio, L. C. Kopel, J. B. Braun, T. L. Gadzikwa, K. L. Hull, R. G. Brisbois, C. J. Markworth and P. A. Grieco, *Org. Lett.*, 2002, **4**, 3199.
31 L. Zhao, R. Ma, J. Li, Y. Li, Y. An and L. Shi, *Biomacromolecules*, 2008, **9**, 2601.
32 H. Yao, K. Domoto, T. Isohashi and K. Kimura, *Langmuir*, 2005, **21**, 1067.
33 I. Struganova, *J. Phys. Chem. A*, 2000, **104**, 9670.
34 K. R. Wang, D. S. Guo, B. P. Jiang, Z. H. Sun and Y. Liu, *J. Phys. Chem. B*, 2010, **114**, 101.
35 J. N. Demas and G. A. Grosby, *J. Phys. Chem.*, 1971, **75**, 991.
36 J. Herbich, C. Y. Hung, R. P. Thummel and J. Waluk, *J. Am. Chem. Soc.*, 1996, **118**, 3508.
37 H. Berber, C. Ogretir, E. C. S. Lekesiz and E. Ermis, *J. Chem. Eng. Data*, 2008, **53**, 1049.
38 J. R. Albani, *Principles and Applications of Fluorescence Spectroscopy*, Blackwell Science, 2007, pp. 79–87.
39 I. M. Kolthoff and M. K. Chantooni Jr, *J. Am. Chem. Soc.*, 1965, **87**, 4428.